The Plant Cell, Vol. 14, 1223–1233, June 2002, www.plantcell.org © 2002 American Society of Plant Biologists

IRT1, an Arabidopsis Transporter Essential for Iron Uptake from the Soil and for Plant Growth

Grégory Vert,[a] Natasha Grotz,[b] Fabienne Dédaldéchamp,[a] Frédéric Gaymard,[a] Mary Lou Guerinot,[b] Jean-François Briat,[a] and Catherine Curie[a,1]

[a] Biochimie et Physiologie Moléculaire des Plantes, Centre National de la Recherche Scientifique (Unité Mixte de Recherche 5004)/Institut National de la Recherche Agronomique/Agro-M/Université Montpellier II, 2 Place Viala, F-34060 Montpellier Cedex 1, France

[b] Department of Biological Sciences, Dartmouth College, Hanover, New Hampshire 03755

Plants are the principal source of iron in most diets, yet iron availability often limits plant growth. In response to iron deficiency, Arabidopsis roots induce the expression of the divalent cation transporter IRT1. Here, we present genetic evidence that IRT1 is essential for the uptake of iron from the soil. An Arabidopsis knockout mutant in *IRT1* is chlorotic and has a severe growth defect in soil, leading to death. This defect is rescued by the exogenous application of iron. The mutant plants do not take up iron and fail to accumulate other divalent cations in low-iron conditions. IRT1–green fluorescent protein fusion, transiently expressed in culture cells, localized to the plasma membrane. We also show, through promoter::β-glucuronidase analysis and in situ hybridization, that *IRT1* is expressed in the external cell layers of the root, specifically in response to iron starvation. These results clearly demonstrate that IRT1 is the major transporter responsible for high-affinity metal uptake under iron deficiency.

INTRODUCTION

Iron is an essential element required for respiration, photosynthesis, and many other cellular functions such as DNA synthesis, nitrogen fixation, and hormone production. Although abundant in nature, iron often is unavailable because it forms insoluble ferric hydroxide complexes in the presence of oxygen at neutral or basic pH (Guerinot and Yi, 1994). In contrast, anaerobic conditions in acidic soils can lead to cellular iron overload, which causes serious damage to plants because free iron catalyzes the formation of reactive oxygen species (Guerinot and Yi, 1994; Briat et al., 1995; Briat and Lebrun, 1999). Therefore, to control their iron homeostasis, multicellular organisms have to balance iron uptake, intracellular compartmentalization, partitioning to the various organs, and storage.

Plants have evolved two main strategies to cope with iron-deficient growth conditions. Grasses release phytosiderophores, which are secondary amino acids synthesized from Met, that chelate Fe(III) in the soil solution (Takagi et al., 1984). We recently reported on the cloning of the *yellow stripe1* (*ys1*) gene that encodes a high-affinity transporter of the Fe(III)-phytosiderophore complex (Curie et al., 2001). Nongrasses, including Arabidopsis, acidify the soil to increase iron solubility, reduce ferric iron at the root surface, and then transport the resulting ferrous iron across the root plasma membrane (Marschner and Röhmeld, 1994). In Arabidopsis, low iron-inducible ferric chelate reduction has been assigned to the product of the *FRO2* gene, one of five Arabidopsis orthologs of the *Saccharomyces cerevisiae FRE1* and *FRE2* genes that encode the plasma membrane–associated ferric-chelate reductase (Robinson et al., 1999).

The identity of the ferrous iron transporter has not been determined unambiguously. Among the known broad-range plant metal transporters, three families, NRAMP, YSL, and ZIP, may be involved in iron transport. Members of the Arabidopsis NRAMP family have been shown to be involved in iron homeostasis (Curie et al., 2000; Thomine et al., 2000); however, their physiological role in the plant remains unclear. Plant NRAMP transporters could be involved in the compartmentalization of metals at the cellular level (Curie et al., 2000; Thomine et al., 2000). Although the Fe(III)-phytosiderophore uptake system is specific to grasses, we recently reported that Arabidopsis also expresses a family of eight *yellow stripe1-like* (*ysL*) genes highly homologous with the maize *ys1* gene (Curie et al., 2001). Because nicotianamine, a precursor of the phytosiderophores, is synthesized by all plants and has iron chelation properties similar to the phytosiderophores, it is likely that iron-nicotianamine complexes, and more generally metal-nicotianamine complexes, are the

[1] To whom correspondence should be addressed. E-mail curie@ensam.inra.fr; fax 33-467-52-57-37.

Article, publication date, and citation information can be found at www.plantcell.org/cgi/doi/10.1105/tpc.001388.

substrates transported by the *ysL* gene products. No functional data are available at present concerning the YSL transporters, although localization of nicotianamine in phloem, and more recently in vacuoles of iron-overloaded cells, suggests that they could be involved in internal metal ion trafficking and iron storage (Stephan and Scholz, 1993; Pich et al., 2001).

IRT1, the founding member of the large ZIP family, was identified as an Arabidopsis cDNA able to functionally complement the *S. cerevisiae fet3fet4* mutant defective in both high- and low-affinity iron uptake (Eide et al., 1996). Expression of *IRT1* in *S. cerevisiae* confers a novel, high-affinity ferrous iron uptake activity as well as enhanced Zn(II) and Mn(II) uptake activities (Eide et al., 1996; Korshunova et al., 1999). The *IRT2* gene, a close homolog of *IRT1* in the ZIP family, also encodes a high-affinity iron transporter (Vert et al., 2001). Expression of both *IRT1* and *IRT2* is induced in roots upon iron starvation (Eide et al., 1996; Vert et al., 2001); thus, IRT1 and IRT2 are likely to be components of the iron-deficiency response of Arabidopsis roots and represent good candidates to perform ferrous iron uptake from the soil.

In this article, we report on the use of a reverse-genetic approach, as well as localization experiments, to determine the in planta function of the IRT1 metal transporter. Isolation of an Arabidopsis *IRT1* knockout mutant allowed us to establish that under iron-deficient conditions, IRT1 is responsible for the majority of the iron uptake activity of the root and also is responsible for the uptake of heavy metals such as zinc, manganese, cobalt, and cadmium.

RESULTS

Isolation and Molecular Characterization of the *irt1-1* Knockout Line

The analysis of mutants is a valuable tool for revealing the role of a particular gene in physiological and developmental processes in plants. Using a reverse-genetic screen (Krysan et al., 1996), we have identified a mutant allele of the Arabidopsis *IRT1* gene. A PCR primer designed to amplify *IRT1* was used in combination with a primer specific to the T-DNA left border. Pooled template DNA was isolated from 25,440 T-DNA–transformed lines generated at the Laboratoire de Génétique et Amélioration des Plantes, Institut National de la Recherche Agronomique (Versailles, France) (Bechtold et al., 1993; Bouchez et al., 1993). The mutant line obtained contained two additional T-DNA insertions that were eliminated by two successive backcrosses. The single-insertion mutant obtained was named *irt1-1*.

Cosegregation of *irt1-1* with the T-DNA was established by PCR. Sequence analysis revealed that the T-DNA is inserted in the third exon of the *IRT1* gene (Figure 1A), 1128 bp downstream of the translation start codon, and that the insertion was accompanied by a 10-bp deletion of the *IRT1* sequence at the integration site. To investigate *IRT1* expression in the knockout, reverse transcriptase–mediated (RT) PCR on total RNA prepared from both wild-type and *irt1-1* iron-starved plants was performed using *IRT1*-specific primers. An amplification product corresponding to *IRT1* was seen in the wild type, whereas no amplification was detected in *irt1-1* (Figure 1B). In addition, protein gel blot analysis was performed on total protein prepared from wild-type and *irt1-1* plants to test for the presence of the IRT1 protein. In the wild type, a strong hybridization signal was seen solely in roots of plants grown under iron-deficient conditions (Figure 1C), which reflects the root-specific iron-deficient induction of *IRT1* transcripts reported previously (Eide et al., 1996). Consistent with the RT-PCR experiment, there was no detectable IRT1 protein in the *irt1-1* mutant (Figure 1C).

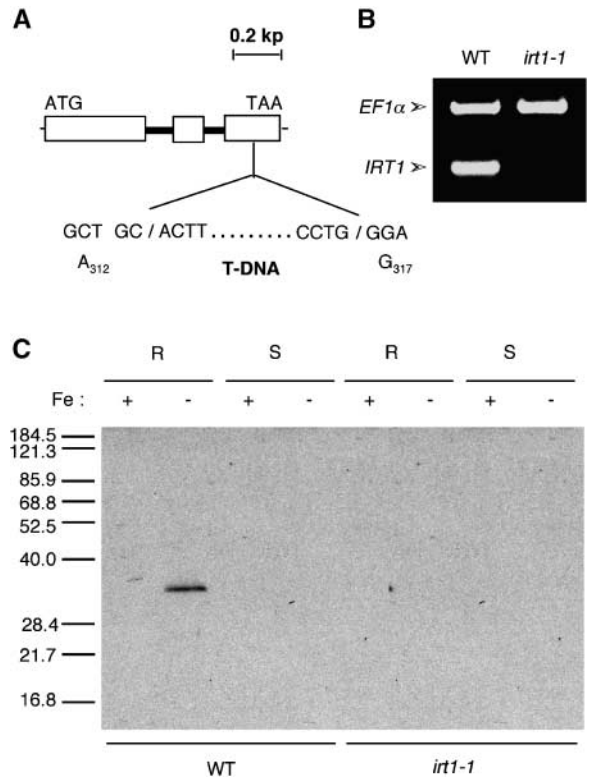

Figure 1. Molecular Characterization of the *irt1-1* Knockout Mutant.

(A) Scheme of the T-DNA integration site in *irt1-1*. The location of the T-DNA insertion within the sequence of the *IRT1* gene is shown. Exons are boxed.

(B) Detection of *IRT1* mRNA. RT-PCR was performed on total RNA extracted from wild-type (WT) and *irt1-1* iron-deficient roots. EF1α-specific primers were included as a control.

(C) Immunoblot analysis of IRT1. Total proteins were extracted from wild-type and *irt1-1* plants grown in the presence (+) or absence (−) of iron. The blot was probed with antibodies directed against IRT1. R, roots; S, shoots.

irt1-1 Exhibits a Lethal Chlorotic Phenotype

The *irt1-1* homozygous mutant showed severe leaf chlorosis in greenhouse conditions compared with wild-type plants (Figure 2). Moreover, these plants did not develop beyond the four- to six-true-leaf stage. They generally developed a short yellow floral stalk producing one to three flowers, with chlorotic sepals, that never developed further into siliques (Figure 2). Such plants, therefore, are sterile and die after 3 to 4 weeks. The *irt1-1* lethal phenotype is rescued when plants are transformed with a functional *IRT1* gene under the control of its own promoter (Figure 2), confirming that the loss of IRT1 is responsible for the chlorotic phenotype of *irt1-1*.

Short-day conditions increased *irt1-1* phenotype severity, and conversely, long-day conditions improved the mutant's growth. Moreover, the heterozygote *irt1-1*+/−, which is morphologically indistinguishable from the wild type (Figure 2) in long days, flowered earlier in short days (data not shown). The fact that plants carrying only one copy of the *IRT1* gene showed abnormal growth in short days emphasizes the importance of the IRT1 transporter in the plant. This correlation between *irt1-1* phenotypic severity and light cycle suggests that IRT1 iron uptake activity is more efficient at night than during the day, so that in plants lacking IRT1, longer nights would result in a stronger deficit of iron uptake.

Figure 2. Phenotype of *irt1-1*.

Phenotype of 15-day-old (top) or 4-week-old (bottom) plants grown in soil. WT, wild-type plant; *irt1-1*, *irt1-1* mutant; *irt1-1* +/−, *irt1-1* heterozygous plant; *irt1-1*:*IRT1*, transgenic *irt1-1* mutant expressing functional *IRT1*; *irt1-1* + Fe, *irt1-1* watered with 0.5 g/L Sequestrene.

IRT1 Is Involved in Iron Homeostasis in Planta

The strong leaf chlorosis seen with *irt1-1* is typical of iron-deficient plants because iron is required for chlorophyll biosynthesis. Therefore, we tested whether supplementing the mutant with iron could reduce its chlorosis. Figure 2 shows that *irt1-1* plants watered with a large excess of Sequestrene (see Methods) appeared green and healthy. Moreover, such iron supplementation allowed *irt1-1* plants to set seeds at levels comparable to those of the wild type (data not shown). These results demonstrate a role for IRT1 in iron homeostasis in planta. Consistent with these findings, leaf iron content of the homozygous *irt1-1* mutant was only 30% of that of the wild type, whereas it was not affected in the heterozygote grown under long-day conditions (Figure 3). When complemented with a functional *IRT1* gene or when supplemented with Sequestrene as described above, *irt1-1* contained nearly wild-type levels of iron in its leaves (Figure 3). Thus, IRT1 is essential to maintain plant iron content and to ensure plant growth and development.

Functional complementation and uptake assays in yeast suggested that IRT1 functions as a high-affinity ferrous iron transporter (Eide et al., 1996). To establish the role of IRT1 in iron absorption by the plant, we compared the accumulation of radiolabeled iron in *irt1-1* and wild-type plants. A total of 10 μM ^{55}Fe-EDTA was provided to roots of 2-week-old plants, and ^{55}Fe content in shoots was monitored 2 days later. When plants were grown in iron-replete medium before the experiment, conditions that repress *IRT1* expression (Eide et al., 1996), both wild-type and *irt1-1* plants accumulated similarly low amounts of ^{55}Fe (Figure 4). Transferring the wild-type plants to a low-iron-containing medium for the last 4 days before the experiment resulted in a large increase in ^{55}Fe accumulation in the shoots. This observation is consistent with the physiological response to iron deficiency (Fox et al., 1996). On the contrary, after iron starvation, *irt1-1* did not show any significant increase in ^{55}Fe accumulation. Therefore, *irt1-1* lost the capacity to accumulate iron under iron-deficient conditions, which strongly supports the idea that IRT1 is the main iron transporter operating in roots of iron-starved plants.

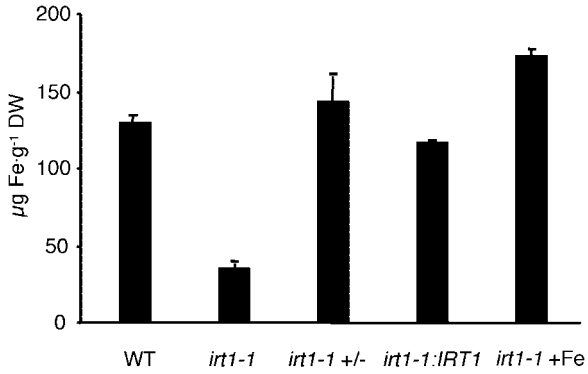

Figure 3. Reduced Leaf Iron Content in *irt1-1*.

Leaf iron content was assessed on 4-week-old plants grown in soil. DW, dry weight; WT, wild-type plant; *irt1-1*, homozygous mutant; *irt1-1* +/−, heterozygous plant; *irt1-1*:*IRT1*, *irt1-1* mutant transformed with a functional *IRT1*; *irt1-1* + Fe, *irt1-1* watered with 0.5 g/L Sequestrene.

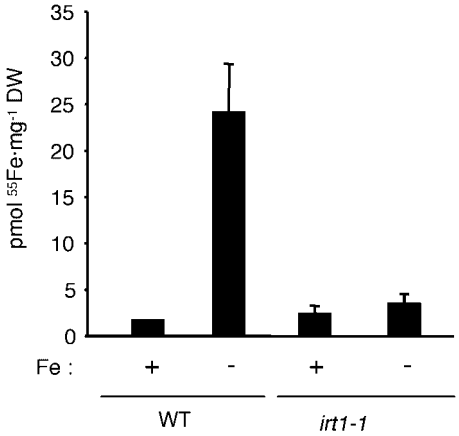

Figure 4. Defect of ^{55}Fe Accumulation in *irt1-1*.

Accumulation of ^{55}Fe was performed on wild-type (WT) and *irt1-1* plants grown in iron-sufficient (+) or iron-deficient (−) conditions for 4 days and incubated for 48 h in the presence of 10 μM ^{55}Fe-EDTA. DW, dry weight.

Iron-Deficiency Responses Are Upregulated in the *irt1-1* Mutant

Because of the defect in the iron status of *irt1-1*, we hypothesized that other known responses of the plant to iron deficiency, including root iron reduction and uptake activities other than IRT1, may be deregulated in the mutant. Figure 5A shows that root ferric reductase activity was higher in the mutant, regardless of the iron content in the medium. At the molecular level, this was reflected by the accumulation of the low-iron-inducible *FRO2* and *IRT2* transcripts (Figure 5B). Although their pattern of accumulation was identical in *irt1-1* and wild-type plants (i.e., upregulated by iron deficiency), the overall amount of *FRO2* and *IRT2* transcripts was increased in the mutant, from ~10-fold in iron-replete conditions (Figures 5B and 5C, +Fe) to ~30-fold in the absence of added iron (Figures 5B and 5C, −Fe).

Thus, both physiological and molecular responses to iron deficiency were enhanced in *irt1-1* compared with wild-type plants, regardless of external iron levels. This general upregulation of the deficiency response, however, failed to compensate for the lack of a functional *IRT1* gene. Accordingly, overexpression of the root iron transporter encoding the *IRT2* gene under the control of the 35S promoter of *Cauliflower mosaic virus* in *irt1-1* did not rescue its phenotype (data not shown). Together, these data further confirm that IRT1 is an essential protein and that it represents a limiting step for iron uptake under iron deficiency.

IRT1 Transports Heavy Metals in Planta

Plants are known to accumulate heavy metals in response to iron starvation (Welch et al., 1993; Cohen et al., 1998). Characterization of IRT1 in yeast showed that in addition to iron, IRT1 also can transport zinc, manganese, cadmium, and probably cobalt (Eide et al., 1996; Korshunova et al., 1999; Rogers et al., 2000). To determine the specificity of IRT1 in planta, we measured the amount of various metals contained in wild-type and *irt1-1* plants. Both plants accumulated the same amount of metals under iron-replete conditions (Figure 6A). When plants were grown under iron deficiency, however, zinc, manganese, and cobalt but not copper increased dramatically in the roots of the wild type but not in *irt1-1* (Figure 6A). Therefore, we investigated whether deficiency in other metal ions could contribute to the *irt1-1* phenotype. Watering plants with zinc, manganese, or cobalt solution did not reverse the chlorotic phenotype (Figure 6B), further indicating that iron deficiency is the major cause of the *irt1-1* phenotype.

Finally, we examined the sensitivity to cadmium to determine whether IRT1 could transport cadmium in planta. Both wild-

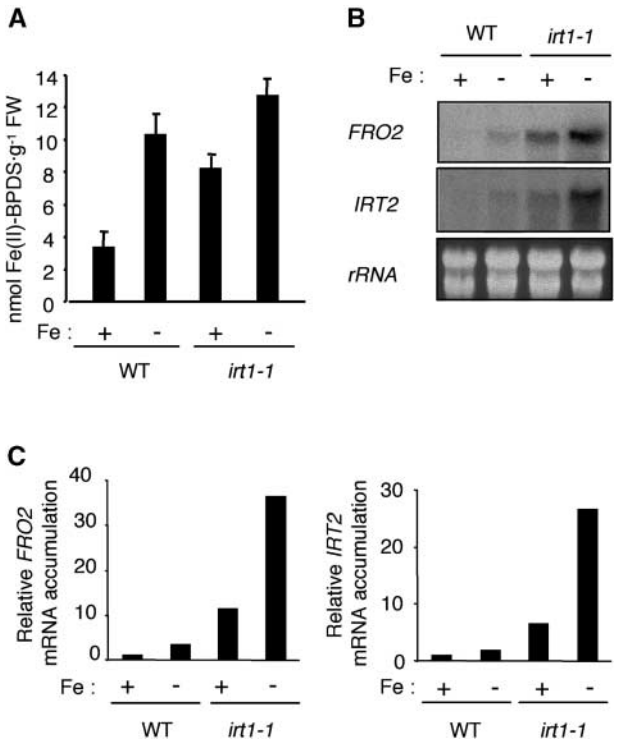

Figure 5. Deregulation of the Iron-Deficiency Responses in *irt1-1*.

(A) Root ferric chelate reductase activity in wild-type (WT) and *irt1-1* plants grown in iron-sufficient (+) or iron-deficient (−) conditions for 4 days. FW, fresh weight.

(B) Expression of iron deficiency–induced genes. Twenty micrograms of total RNA extracted from wild-type or *irt1-1* roots of plants grown in iron-sufficient or iron-deficient conditions for 3 days was blotted and hybridized with *FRO2* and *IRT2* cDNA probes.

(C) Quantification relative to the 25S rRNA of the RNA gel blots presented in **(B)**.

type and *irt1-1* plants appeared resistant to toxic amounts of cadmium when grown in iron-sufficient conditions (Figure 7A). Under low-iron conditions, only *irt1-1* plants were chlorotic. However, the addition of cadmium to iron-deficient plants had no further effect on the *irt1-1* mutant, whereas a dramatic chlorosis developed in the wild type. This observation probably was the result of the competition between the excess cadmium and iron present in trace amounts in the medium. Whether cadmium enters the plant was determined by measuring the cadmium content of plants grown with cadmium and low iron. Figure 7B shows that *irt1-1* roots contained five times less cadmium than the wild type. Thus, IRT1 transports iron, zinc, manganese, and cobalt but not copper in Arabidopsis roots and can mediate cadmium uptake from the environment.

IRT1 Is a Plasma Membrane Transporter

The PsortI (Nakai and Kanehisa, 1992) and TargetP (Emanuelsson et al., 2000) programs predicted a plasma membrane localization of the IRT1 protein. To examine the localization experimentally, we fused green fluorescent protein (GFP) to the C terminus of IRT1 for expression of the corresponding protein in living cells. Protoplasts made from an Arabidopsis cell suspension culture were transfected with constructs to transiently express either GFP or IRT1-GFP under the control of the 35S promoter of *Cauliflower mosaic virus*. Green fluorescence from IRT1-GFP localized to a thin layer surrounding a nonfluorescent cytoplasm, as indicated by the presence of chloroplasts in a black nonfluorescent background. In contrast, fluorescence corresponding to GFP alone was localized in the cytoplasm and in the nucleus (Figure 8C). These results confirmed that IRT1 is targeted to the plasma membrane in vivo, in agreement with its role in iron uptake.

IRT1 Is Expressed in the Root Epidermis

Because this and previous studies (Eide et al., 1996) suggest a role of IRT1 in iron uptake from the rhizosphere across the plasma membrane of the root epidermal cells, we next investigated the localization of *IRT1* expression to confirm its physiological role. Transgenic plants expressing the *uidA* gene, which encodes β-glucuronidase (GUS), under the control of the *IRT1* promoter were generated to determine accurately the tissue localization of *IRT1* promoter activity. Enzymatic analysis of GUS expression indicated that the *IRT1* promoter was >100-fold more active in roots than in shoots (data not shown). GUS activity in roots was induced by iron deficiency, from 2.2 to 35.3 nmol methylumbelliferone·min^{-1}·μg^{-1} protein (Figure 9A), with an average induction factor of 16.5, consistent with the value of induction of *IRT1* expression established using RNA gel blot hybridization (Vert et al., 2001). GUS activity in shoots, although weak, also increased ~10-fold in response to iron deficiency (data not shown).

We then assayed GUS histochemical staining on either

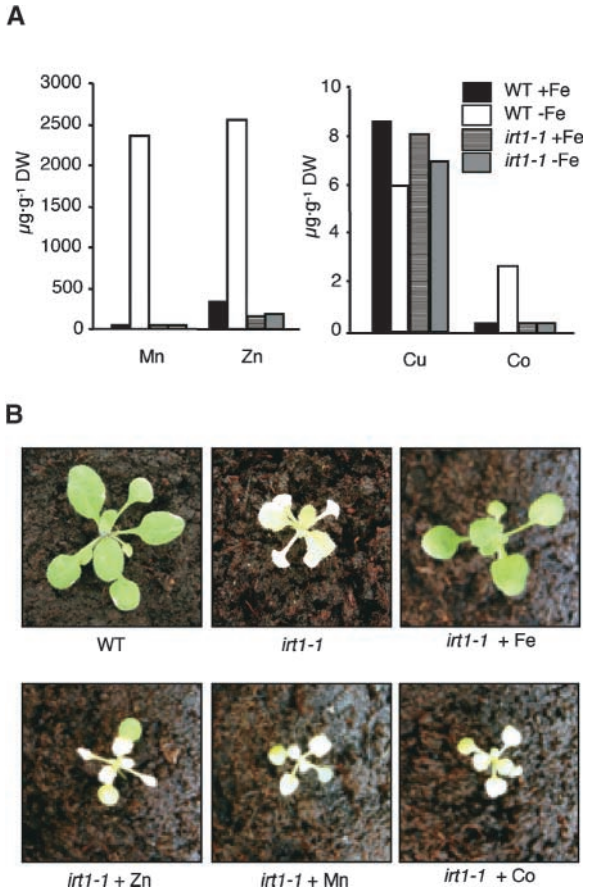

Figure 6. IRT1 Is a Multispecific Metal Ion Transporter in Planta.

(A) Elemental analysis of wild-type (WT) and *irt1-1* roots. Plants were grown in the presence (+Fe) or absence (−Fe) of iron for 5 days, and roots were processed for inductively coupled plasma mass spectrometry analysis (see Methods). DW, dry weight.

(B) Phenotype of 15-day-old wild-type and *irt1-1* plants grown in soil and irrigated either with water (wild type and *irt1-1*) or with a solution of 600 μM Sequestrene (*irt1-1* + Fe), 500 μM $ZnCl_2$ (*irt1-1* + Zn), 500 μM $MnCl_2$ (*irt1-1* + Mn), or 50 μM $CoCl_2$ (*irt1-1* + Co) as indicated.

iron-sufficient (Figure 9B) or iron-deficient (Figures 9C to 9F) plants. Consistent with the results of RNA and protein gel blot experiments, we did not detect GUS staining in iron-sufficient plants (Figure 9B) or in shoots of iron-deficient plants (Figure 9C). However, roots of iron-deficient plants showed strong staining, except for the meristematic zone (Figures 9D and 9E). GUS activity was located in the outer tissues of the root, including root hairs, epidermis, and to a lesser extent cortex (Figures 9D to 9F). We showed previously a very similar pattern of expression for *IRT2* promoter–GUS fusions, except that staining was restricted to the subapical zone of the root (Vert et al., 2001), whereas this study indicates that *IRT1* promoter–driven GUS activity extended up to the lateral branching zone (Figure 9E). However, because the *IRT1* promoter was ~100-fold stronger than the

IRT2 promoter, it is possible that GUS staining in the lateral branching zone of *IRT2-GUS*–expressing roots is under the threshold of detection. In situ hybridization analysis on longitudinal sections of iron-deficient roots indicated that *IRT1* mRNA was present mainly in the epidermal cells of the root (Figure 9G). No signal was observed upon hybridization with the *IRT1* sense probe (Figure 9H). Thus, we observed colocalization of the *IRT1* mRNA with the *IRT1* promoter activity in the root epidermis, which is consistent with a role of IRT1 in iron absorption from the soil solution.

IRT1 Is Expressed in Flower

The expression of *IRT1* in other plant organs was investigated by RNA gel blot analysis on total RNA prepared from soil-grown plants. *IRT1* mRNA was not detected in rosette leaves, cauline leaves, stems, or siliques (Figure 10A). However, in addition to roots, as described previously (Eide et al., 1996), *IRT1* transcripts accumulated in flowers (Figure 10A). To further investigate the role of IRT1 in flowers, we examined the level of IRT1 transcripts before and after pollination. *IRT1* mRNA accumulated before pollination and decreased strongly thereafter (Figure 10B), excluding a possible role in seed loading. Moreover, histochemical staining of flowers of transgenic plants expressing the *IRT1* promoter–GUS fusion showed GUS staining exclusively in the anther filament (Figures 10C and 10D). This result suggests that IRT1 could be involved in providing iron to maturing pollen grains and is consistent with it being transcribed specifically in unpollinated flowers. Indeed, a requirement for iron by pollen grains is inferred from the accumulation of ferritin, the iron storage protein, in maize pollen (J.-F. Briat, unpublished results).

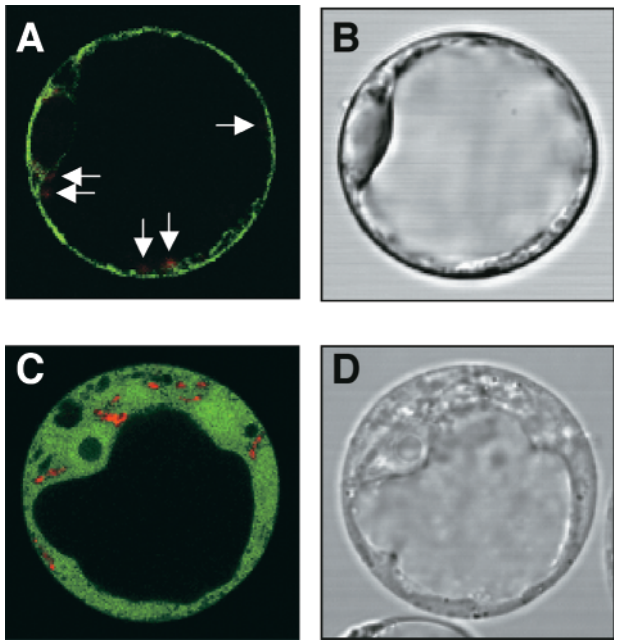

Figure 8. Subcellular Localization of the IRT1 Protein.

Subcellular localization of IRT1-GFP **(A)** and GFP alone **(C)** in transfected Arabidopsis protoplasts. Chlorophyll autofluorescence, shown in red (indicated by arrows in **[A]**), is superimposed on GFP fluorescence in **(A)** and **(C)**. **(B)** and **(D)** show the transmission view of the same fields shown in **(A)** and **(C)**, respectively.

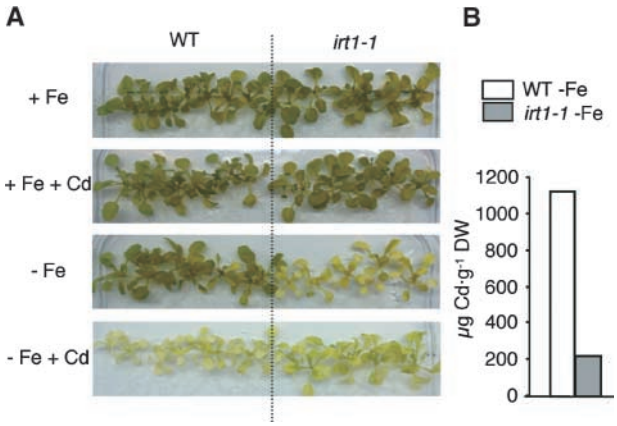

Figure 7. Reduced Cadmium Sensitivity of *irt1-1*.

(A) Phenotype of wild-type (WT) and *irt1-1* plants grown in the presence of cadmium. Plants were grown in the presence or absence of iron (+Fe and −Fe) and in the presence or absence of 20 μM cadmium (+Cd and −Cd) for 8 days.

(B) Cadmium content in roots of the iron-deficient plants described in **(A)** and processed for inductively coupled plasma mass spectrometry analysis. DW, dry weight.

To discriminate between developmentally driven and iron deficiency–driven expression of *IRT1* in flowers, we next tested the influence of iron nutrition on the accumulation of *IRT1* transcripts. Control plants grown in soil were compared with plants watered with an excess of iron (0.5 g/L Sequestrene). RNA gel blot hybridization on total RNA extracted from these plants revealed *IRT1* transcripts in control plants but not in iron-supplemented plants, confirming the iron-deficient and iron-sufficient status, respectively, of these plants (Figure 10E). Interestingly, however, *IRT1* mRNA accumulated in flowers regardless of plant iron status (Figure 10E). We conclude from these data that *IRT1* expression in stamens corresponds to a developmental need rather than to a response to iron nutritional status, as is the case in roots.

DISCUSSION

The data presented here offer insight into a molecular pathway of iron uptake in dicotyledonous plants. Although additional iron uptake pathways may exist, this work pro-

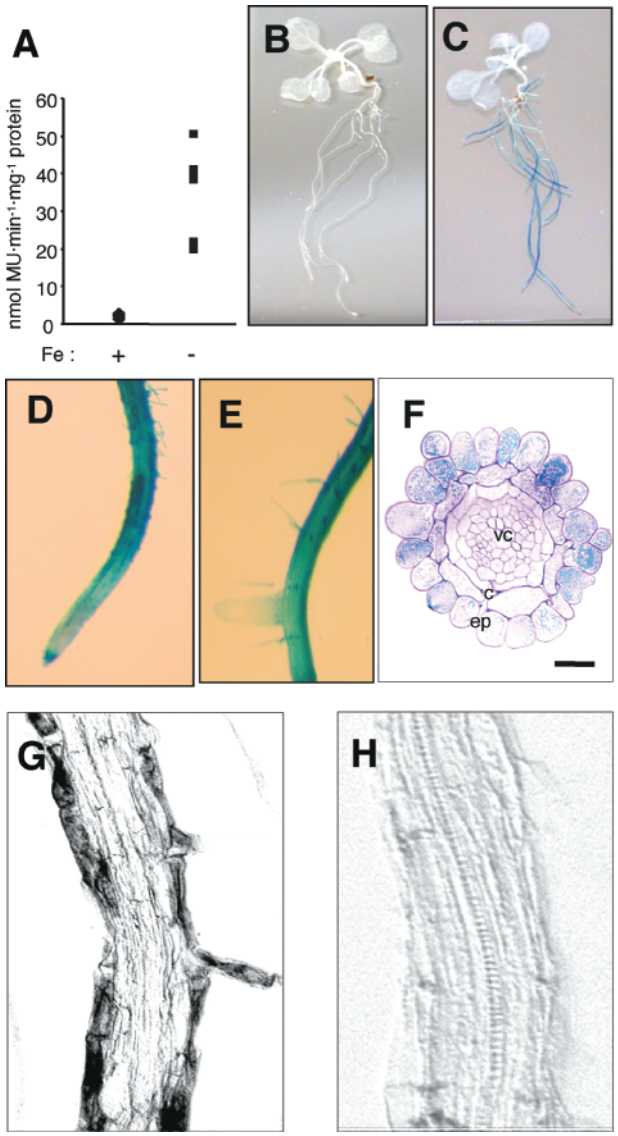

Figure 9. Root Periphery Localization of *IRT1* Expression.

(A) Enzymatic GUS assay was performed on six independent transgenic lines expressing an *IRT1* promoter–GUS fusion protein and grown in the presence of 50 μM Fe-EDTA (+Fe) or in the absence of added iron (−Fe). No significant GUS activity was detected in wild-type plants (data not shown). MU, methylumbelliferone.

(B) to **(F)** GUS histochemical staining of the transgenic lines.

(B) Twelve-day-old plantlets grown as in **(A)** in the presence of iron.

(C) Twelve-day-old plantlets grown as in **(A)** in the absence of iron.

(D) and **(E)** Enlargement of the iron-deficient roots shown in **(C)** to highlight the weak GUS staining in the meristematic zone **(D)** and the strong staining in the root hairs and in the root lateral branching zone **(E)**.

(F) Three-micrometer cross-section of an iron-deficient root shown in **(C)**. Cross sections were counterstained with Schiff dye. c, cortex; ep, epidermis; vc, vascular cylinder. Bar = 100 μm.

(G) In situ hybridization experiments were performed on longitudinal sections (10 μm) of iron-deficient roots using an *IRT1* antisense probe.

(H) In situ hybridization experiments were performed on longitudinal sections (10 μm) of iron-deficient roots using a sense probe.

vides strong evidence that IRT1 is the major root iron uptake system in soil. First, a null allele of *IRT1* was lethal. Second, the important reduction in iron accumulation in the *irt1-1* mutant, even though both ferric chelate reductase activity and *IRT2* expression were enhanced, indicates that no biochemical activity in the root can compensate for the loss of IRT1. Nevertheless, fertilization with a large amount of iron (0.5 g/L Sequestrene) reversed the *irt1-1* chlorotic phenotype (Figure 2). Therefore, the low-affinity transport systems that are known to operate under iron-sufficient conditions (Fox et al., 1996), although uncharacterized at the molecular level, must compensate for the loss of IRT1. Third, the accumulation of zinc, manganese, cobalt, and cadmium under iron starvation was lost or greatly reduced in *irt1-1* plants. This finding suggests that even though some ZIP and NRAMP proteins may be involved in the uptake of metal ions such as zinc, manganese, and cadmium (Grotz et al., 1998; Curie et al., 2000; Thomine et al., 2000; Vert et al., 2001), the accumulation of heavy metals observed in response to iron deficiency (Welch et al., 1993; Cohen et al., 1998) is mediated primarily by IRT1.

We failed to measure reproducible short-term ^{55}Fe uptake in the roots, both in the wild type and in *irt1-1*, because of nonspecific iron binding to the roots leading to a high background (data not shown). However, we measured a strong reduction in ^{55}Fe accumulation in the shoots of *irt1-1* over 48 h (Figure 4). In addition to a defect in root iron uptake, a defect in iron translocation from roots to shoots also could produce a similar result. However, we have shown that in roots, *IRT1* is expressed highly and exclusively in the outer layers under iron-limited conditions (Figure 9). Furthermore, an IRT1-GFP fusion protein was targeted to the plasma membrane of cell suspension protoplasts (Figure 8). These results exclude a role for IRT1 in iron translocation and allows us to conclude unambiguously that IRT1 functions in iron absorption from the soil.

Why does IRT1 mediate the accumulation of other metals? IRT1-mediated accumulation of zinc, manganese, and cobalt may be physiologically relevant because, to some extent, other divalent metal cations are known to replace iron in some cellular processes under low-iron conditions. During heme biosynthesis, for instance, low-iron conditions stimulate zinc chelation by protoporphyrin in bovine liver (Taketani and Tokunaga, 1982; Bloomer et al., 1983). Knocking out the *IRT1* gene led to a strong decrease in zinc, manganese, and cobalt contents in the roots of the mutant in low-iron conditions (Figure 6). We determined whether this alteration of zinc homeostasis in the mutant could lead to deregulation of the *ZIP* genes potentially involved in zinc transport. We failed to detect an enhanced expression in *irt1-1* of *ZIP1* and *ZIP3* (data not shown), which are known

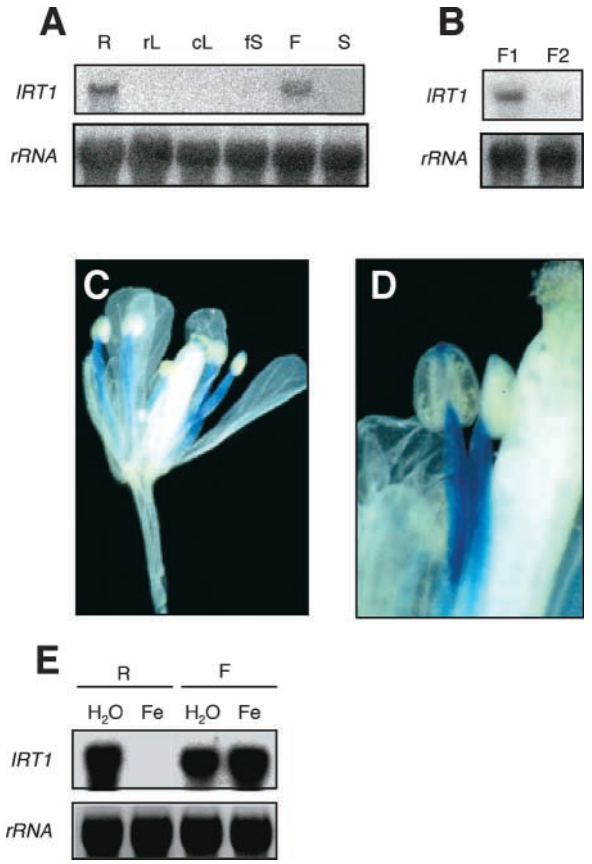

Figure 10. *IRT1* Expression in Flower.

(A) Spatial distribution of *IRT1* expression using 10 μg of total RNA isolated from roots (R), rosette leaves (rL), cauline leaves (cL), floral stalk (fS), flowers (F), and siliques (S) of 6-week-old soil-grown plants.

(B) Developmental analysis of *IRT1* expression in flowers using 10 μg of total RNA extracted from flowers of 6-week-old plants before pollination (F1) and after pollination (F2).

(C) and **(D)** Histochemical localization of GUS activity in flowers of 6-week-old GUS transgenic plants grown in soil.

(C) Flower.

(D) Enlarged view of a stained anther filament.

(E) Analysis of *IRT1* expression in response to iron status. Gel blot analysis was performed using 15 μg of total RNA isolated from roots (R) and flowers (F) of 6-week-old plants irrigated with either water (H_2O) or 0.5 g/L Sequestrene (Fe).

to be upregulated in response to zinc starvation (Grotz et al., 1998). Although we cannot exclude the possibility that other ZIP members might give a different result, this finding suggests that the decrease in zinc content in the mutant is not sufficient to deregulate plant zinc homeostasis and to stimulate its zinc-deficiency response.

More than 30 genes encode putative metal transporters in the Arabidopsis genome. Although IRT1 plays a key role in iron uptake, IRT2 also is a good candidate for iron acquisition from the soil. Indeed, expression of the *IRT2* gene is inducible by iron starvation, and *IRT2* promoter activity is specific to the most external cell layers of the roots (Vert et al., 2001). The fact that the two high-affinity iron transporters IRT1 and IRT2 share the same territories of expression in the root in response to the same signal raises the question of their redundancy. Upregulation of *IRT2* observed in the *irt1-1* mutant (Figure 5B) failed to rescue its chlorotic phenotype (Figure 2), suggesting either that these two transporters have distinct transport activities in root epidermis or that the level of expression of *IRT2* in the mutant is not sufficient. The latter hypothesis was disproved by the generation of *irt1-1*/35S::IRT2 transgenic plants that failed to improve the *irt1-1* phenotype. Alternatively, IRT2 may be localized on an intracellular membrane. In that case, IRT2 may act as an intracellular relay for IRT1. Upon iron starvation, the rapid and massive activation of IRT1 leading to iron uptake from root epidermal cells is likely to provoke local excess accumulation of iron in the cytoplasm. This iron shock must be controlled, through compartmentalization via other iron transporters, to avoid iron toxicity. Such a model has been proposed for zinc transport in yeast (MacDiarmid and Eide, 2001). This and previous work led us to propose that IRT1 is the major high-affinity iron transporter in Arabidopsis and also is responsible for metal uptake from the soil solution under iron deficiency.

METHODS

Identification of the *irt1-1* Knockout Mutant

Mutant *Arabidopsis thaliana* lines (ecotype Wassilewskija) containing random T-DNA insertions were screened using PCR as described previously (Krysan et al., 1996). A PCR primer designed to amplify the wild-type gene was used in combination with a T-DNA–specific primer to detect insertions within the *IRT1* gene. The primers used in this screen were IRT1-specific primer (5′-GTTAAGCCCATTTGGCGATAATCGACATTC-3′) and T-DNA left border–specific primer (5′-CTACAAATTGCCTTTTCTTATCGAC-3′). Insertion was verified by DNA gel blot hybridization and sequencing.

Plant Material and Growth Conditions

Plants were cultivated on soil (Humin substrate N2 Neuhaus; Klasmann-Deilmann, Geeste, Germany) in a greenhouse at 23°C and irrigated with either water or 0.5 g/L Sequestrene (~600 μM; Fertiligene, Ecully, France).

For ^{55}Fe accumulation, ferric reductase activity, and RNA gel blot experiments on both wild-type and *irt1-1* plants, seeds of Arabidopsis were surface-sterilized and grown hydroponically in Magenta boxes in the presence of Suc (Touraine and Glass, 1997). During 15 to 20 days of culture at 20°C under short-day conditions (8 h at 150 $\mu E \cdot m^{-2} \cdot s^{-1}$), the medium was changed regularly to allow optimal development. Plant roots then were washed with 2 mM $CaSO_4$ before transfer to either iron-sufficient (50 μM NaFe-EDTA)

or iron-deficient (iron omitted) medium for the periods indicated in the figure legends.

For immunoblot analysis and heavy metal content determination, plants were grown on agar plates containing half-strength Murashige and Skoog (1962) medium up to the four- to six-leaf stage and then transferred to either iron-sufficient (50 μM NaFe-EDTA) or iron-deficient (300 μM Ferrozine [3-(2-pyridyl)-5,6-diphenyl-1,2,4-triazine sulfonate]; Sigma, Saint Louis, MO) medium for 3 days (immunoblot) or 5 days (heavy metal content). For cadmium measurements, plants were grown and transferred as described above, but 20 μM $CdCl_2$ was added, or omitted, to iron-sufficient or iron-deficient plates, respectively. Cadmium sensitivity and content were assessed after 8 days.

β-Glucuronidase (GUS) transgenic plants were grown on plates in half-strength Murashige and Skoog (1962) medium containing 50 μg/mL kanamycin. After 7 days, transformants were transferred to either iron-sufficient (50 μM NaFe-EDTA) or iron-deficient (300 μM Ferrozine) medium and cultivated for 5 more days before GUS assays were performed.

Plasmid Construction and Plant Transformation

DNA manipulations were performed according to standard methods (Sambrook et al., 1989). Transgenic *irt1-1* plants expressing functional *IRT1* were generated by transformation of the mutant with a plasmid containing a 2.5-kb *IRT1* genomic fragment including 1 kb of upstream sequences cloned in the KpnI and XbaI sites of pBibHygro. Arabidopsis transgenic plants (ecotype Columbia) expressing the *IRT1* promoter–GUS fusion were obtained essentially as described previously (Vert et al., 2001), except that 1 kb of the *IRT1* promoter, obtained by PCR, was cloned. The MP90 strain of *Agrobacterium tumefaciens* was used to transform Arabidopsis according to the floral dip protocol (Clough and Bent, 1998). Seeds obtained from the primary transformants were germinated on antibiotic-containing plates, and analyses were performed on the resistant plants (T2).

For IRT1–green fluorescent protein (GFP) fusion, *IRT1* cDNA sequence was amplified by PCR using primers IRT1-GFP-F (5′-GCTCTAGAGCATGAAAACAATCTTCCTCGTAC) and IRT1-GFP-R (3′-CGGGATCCGTTTAGCCCATTTGGCGATAATC). Care was taken to substitute the stop codon TAA of *IRT1* with AAA, encoding for a Lys residue, to fuse IRT1 in frame with the GFP sequence. The *IRT1* PCR product was cloned in the BamHI and XbaI sites of the pBI-GFP vector to fuse the GFP sequence 3′ of the IRT1 sequence under the control of the 35S promoter of *Cauliflower mosaic virus*.

Isolation of Protein and Protein Gel Blot Analysis

Total protein was prepared from both wild-type and *irt1-1* plants grown either in iron-replete or iron-deplete conditions. Extracts were prepared by grinding tissues on ice in extraction buffer (50 mM Tris, pH 8.0, 5% glycerol, 4% SDS, 1% polyvinylpolypyrrolidone, and 1 mM phenylmethylsulfonyl fluoride), followed by centrifugation at 4°C for 15 min at 14,000*g*. Ten micrograms of total protein extracts was resolved on a SDS–polyacrylamide gel, and the immunoblot was probed with an affinity-purified IRT1 antibody (1:1000 dilution). The IRT1 polyclonal antibody was raised in rabbits against a synthetic peptide (PANDVTLPIKEDDSSN) that corresponds to amino acids 170 to 185 of the IRT1 deduced protein sequence and is unique to IRT1 (Quality Controlled Biochemicals, Hopkinton, MA).

Gene Expression

Total RNA was extracted (Lobreaux et al., 1992) from organs of plants cultivated as described above. Samples of RNA were denatured and electrophoresed on a 1.2% 3-(*N*-morpholino)-propanesulfonic acid/formaldehyde/agarose gel before transfer to a nylon membrane (Biotrans; ICN, Irvine, CA). The same blot was hybridized sequentially with probes made from *IRT2* and *FRO2* cDNA. Filters were exposed to a PhosphorImager screen (Kodak) for 72 and 24 h for IRT2 and FRO2, respectively, and signal was revealed using a PhosphorImager (Molecular Dynamics, Sunnyvale, CA). Quantification was performed relative to the 25S rRNA hybridization signal.

Reverse transcriptase–mediated PCR experiments were performed on 5 μg of total RNA treated previously with RNase-free DNase and extracted from iron-deficient wild-type and *irt1-1* plants. The specific primers used for *IRT1* detection were designed to amplify a 181-bp region upstream of the T-DNA insertion to detect possible truncated *IRT1* products in the mutant. Primers used for *IRT1* were IRT1-0 (5′-CATGAAAACAATCTTCCTCGTACTCATTTTTGTC-3′) and IRT1-1 (5′-GAGGAGCTCCAACACCAATC-3′). The internal standard EF1α used in reverse transcriptase–mediated PCR experiments was amplified as a 715-bp product with the specific primers TEFA1 F (5′-ATGGGTAAAGAGAAGTTTCACATC-3′) and TEFA1 R (5′-ACCAATCTTGTAGACATCCTGAAG-3′).

Ferric Chelate Reductase Activity

Root ferric chelate reductase activity in wild-type and *irt1-1* plants was determined with bathophenantrolinedisulfonate to chelate reduced iron, as described (Robinson et al., 1997). Reduction rates were calculated from the absorption of the Fe(II)-bathophenantrolinedisulfonate complex at 535 nm (molar extinction coefficient, 22.14 $M^{-1} \cdot cm^{-1}$). Each value is the mean of three experiments.

^{55}Fe Accumulation

Accumulation experiments were performed using wild-type and *irt1-1* plants grown under iron deficiency or iron sufficiency for 4 days. Roots were washed for 1 min in iron-deficient growth medium and transferred to accumulation medium (iron-free growth medium containing 10 μM Fe-EDTA, 10 μM EDTA, and 0.3 μCi/mL $^{55}FeCl_3$ [DuPont–New England Nuclear, Boston, MA]) and grown for 48 h before harvesting. Shoots were harvested, rinsed in water, dried overnight at 70°C, and weighed, and their radioactivity was measured using a scintillation counter. Each value is the mean of three experiments.

Metal Ion Content

The iron concentration in leaves was determined for soil-grown plants as described (Lobreaux and Briat, 1991). Heavy metal content (zinc, manganese, cobalt, copper, and cadmium) also was determined for both wild-type and *irt1-1* plants grown on plates. Samples were washed for 5 min in a solution containing 5 mM $CaSO_4$ and 10 mM EDTA, dried overnight at 70°C, and weighed, and then 1 g of dry tissue was digested completely in 70% HNO_3 at 120°C. Trace elements were analyzed by inductively coupled plasma mass spectrometry at the University of Montpellier II, and measurements were performed using a PQ II Turbo+ quadrupole inductively coupled

plasma mass spectrometer (VG Elemental, Cambridge, UK). Before analysis, solutions were diluted by a factor of ~100, and indium and bismuth were added to aliquots of the solutions as internal standards for drift correction.

GUS Expression Analyses

Quantification of IRT1 Promoter Activity

For GUS assays, roots and shoots of six kanamycin-resistant T2 lines were harvested separately and ground directly in Eppendorf tubes in 600 μL of GUS extraction buffer (Jefferson et al., 1987). GUS activity was measured fluorometrically using 1 mM 4-methylumbelliferyl-β-D-glucuronide as a substrate (Jefferson et al., 1987). Total protein content of the samples was determined according to Bradford (1976) and used to correct the GUS activity.

Localization of IRT1 Expression

GUS histochemical staining was performed on either 12-day-old plantlets grown on plates or flowers of 6-week-old plants grown in soil using 5-bromo-4-chloro-3-indolyl β-D-glucuronide as a substrate (Jefferson et al., 1987). Stained roots were embedded in hydroxyethylmethacrylate (Technovit 7100; Heraus-Kulzer, Wehrheim, Germany) before cutting thin cross-sections (3 μM) using a Leica RM 2165 microtome (Wetzlar, Germany). Cross-sections were counterstained with Schiff dye and observed with an Olympus BH2 microscope (Tokyo, Japan).

In Situ Hybridization

The plasmid pIRT-1 (Eide et al., 1996) was used to generate sense and antisense probes for in situ hybridization. Sense and antisense probes were labeled with digoxigenin–11-UTP (Roche Molecular Biochemicals, Indianapolis, IN) according to the manufacturer's protocol. For sense probes, pIRT-1 was linearized with SacII and transcribed with T7 RNA polymerase. For antisense probes, pIRT-1 was linearized with XbaI and transcribed with T3 RNA polymerase. Tissue samples were fixed and embedded as described (Di Laurenzio et al., 1996), with the exception that the tissue was embedded in 1% agarose after the 70% ethanol dehydration step. In situ hybridization was performed according to previous protocols (Long et al., 1996; Long and Barton, 1998).

IRT1-GFP Fusion Protein Localization

An Arabidopsis cell suspension culture (Axelos et al., 1992) was transfected using a polyethylene glycol protocol derived from Schirawski et al. (2000). To observe the GFP fluorescence in transfected protoplasts, a Bio-Rad 1024 confocal laser scanning microscope system coupled to a Nikon Optiphot II upright microscope and an argon-krypton ion laser (15 megawatt) was used (Tokyo, Japan). Excitation wavelength was 488 nm for fluorescein isothiocyanate excitation, and emission filters were 520/30 nm for GFP fluorescence and 680/32 nm for chlorophyll autofluorescence. Observation was performed using a Nikon ×20 objective (numerical aperture, 0.75).

ACKNOWLEDGMENTS

The authors thank D. Bouchez (Génétique et Amélioration des Plantes, Institut National de la Recherche Agronomique [INRA], Versailles, France) for providing access to the library of T-DNA–tagged Arabidopsis lines, O. Bruguier (Institut des Sciences de la Terre, de l'Eau et de l'Espace de Montpellier, University of Montpellier, France) for assistance in inductively coupled plasma mass spectrometry analysis, N. Grignon (Biochimie et Physiologie Moléculaire des Plantes, INRA, Montpellier, France) for technical help in root cross-sections and GUS histochemical observations, and Nicole Lautrédou-Audouy (Centre Régional d'Imagerie Cellulaire, Institut National de la Santé et de la Recherche Médicale, Montpellier, France) for help with confocal microscopy observation. The authors thank S. Lobréaux and B. Touraine (BPMP, INRA, Montpellier, France) for providing the pBib-Hygro and pBI-GFP vectors and for technical help in protoplast preparation and transfection. The work of G.V. is supported by a Bourse de Docteur Ingénieur fellowship awarded by the Centre National de la Recherche Scientifique. Research was supported in part by an Action Concertée Incitative (2000-51) from the French Ministry of National Education, Research, and Technology to J.-F.B. and by a grant from the U.S. Department of Energy to M.L.G.

Received December 27, 2001; accepted March 1, 2002.

REFERENCES

Axelos, M., Curie, C., Mazzolini, L., Bardet, C., and Lescure, B. (1992). A protocol for transient expression in *Arabidopsis thaliana* protoplasts isolated from cell suspension culture. Plant Physiol. Biochem. **30,** 123–128.

Bechtold, N., Ellis, J., and Pelletier, G. (1993). *In planta Agrobacterium*-mediated gene transfer by infiltration of adult *Arabidopsis thaliana* plants. C. R. Acad. Sci. Paris **316,** 1194–1199.

Bloomer, J.R., Reuter, R.J., Morton, K.O., and Wehner, J.M. (1983). Enzymatic formation of zinc-protoporphyrin by rat liver and its potential effect on hepatic heme metabolism. Gastroenterology **85,** 663–668.

Bouchez, D., Camilleri, C., and Caboche, M. (1993). A binary vector based on Basta resistance for in planta transformation of *Arabidopsis thaliana*. C. R. Acad. Sci. Paris **316,** 1188–1193.

Bradford, M.M. (1976). A rapid and sensitive method for the quantitation of microgram quantities of protein utilizing the principle of protein-dye binding. Anal. Biochem. **72,** 248–254.

Briat, J.F., Fobis-Loisy, I., Grignon, N., Lobréaux, S., Pascal, N., Savino, G., Thoiron, S., von Wiren, N., and Van Wuytswinkel, O. (1995). Cellular and molecular aspects of iron metabolism in plants. Biol. Cell **84,** 69–81.

Briat, J.F., and Lebrun, M. (1999). Plant responses to metal toxicity. C. R. Acad. Sci. Paris **322,** 43–54.

Clough, S.J., and Bent, A.F. (1998). Floral dip: A simplified method for Agrobacterium-mediated transformation of *Arabidopsis thaliana*. Plant J. **16,** 735–743.

Cohen, C.K., Fox, T.C., Garvin, D.F., and Kochian, L.V. (1998). The role of iron-deficiency stress responses in stimulating heavy-metal transport in plants. Plant Physiol. **116,** 1063–1072.

Curie, C., Alonso, J.M., Le Jean, M., Ecker, J.R., and Briat, J.F.

(2000). Involvement of NRAMP1 from *Arabidopsis thaliana* in iron transport. Biochem. J. **347,** 749–755.

Curie, C., Panaviene, Z., Loulergue, C., Dellaporta, S.L., Briat, J.F., and Walker, E.L. (2001). Maize yellow stripe1 encodes a membrane protein directly involved in Fe(III) uptake. Nature **409,** 346–349.

Di Laurenzio, L., Wysocka-Diller, J., Malamy, J.E., Pysh, L., Helariutta, Y., Freshour, G., Hahn, M.G., Feldmann, K.A., and Benfey, P.N. (1996). The SCARECROW gene regulates an asymmetric cell division that is essential for generating the radial organization of the Arabidopsis root. Cell **86,** 423–433.

Eide, D., Broderius, M., Fett, J., and Guerinot, M.L. (1996). A novel iron-regulated metal transporter from plants identified by functional expression in yeast. Proc. Natl. Acad. Sci. USA **93,** 5624–5628.

Emanuelsson, O., Nielsen, H., Brunak, S., and von Heijne, G. (2000). Predicting subcellular localization of proteins based on their N-terminal amino acid sequence. J. Mol. Biol. **300,** 1005–1016.

Fox, T.C., Shaff, J.E., Grusak, M.A., Norwell, W.A., Chen, Y., Chaney, R.L., and Kochian, L.V. (1996). Direct measurement of ^{59}Fe-labeled Fe^{2+} influx in roots of *Pisum sativum* using a chelator buffer system to control free Fe^{2+} in solution. Plant Physiol. **111,** 93–100.

Grotz, N., Fox, T., Connolly, E., Park, W., Guerinot, M.L., and Eide, D. (1998). Identification of a family of zinc transporter genes from Arabidopsis that respond to zinc deficiency. Proc. Natl. Acad. Sci. USA **95,** 7220–7224.

Guerinot, M.L., and Yi, Y. (1994). Iron: Nutritious, noxious, and not readily available. Plant Physiol. **104,** 815–820.

Jefferson, R.A., Kavanagh, T.A., and Bevan, M.W. (1987). GUS fusions: Beta-glucuronidase as a sensitive and versatile gene fusion marker in higher plants. EMBO J. **6,** 3901–3907.

Korshunova, Y.O., Eide, D., Clark, W.G., Guerinot, M.L., and Pakrasi, H.B. (1999). The IRT1 protein from *Arabidopsis thaliana* is a metal transporter with a broad substrate range. Plant Mol. Biol. **40,** 37–44.

Krysan, P.J., Young, J.C., Tax, F., and Sussman, M.R. (1996). Identification of transferred DNA insertions within Arabidopsis genes involved in signal transduction and ion transport. Proc. Natl. Acad. Sci. USA **93,** 8145–8150.

Lobreaux, S., and Briat, J.F. (1991). Ferritin accumulation and degradation in different organs of pea (*Pisum sativum*) during development. Biochem. J. **274,** 601–606.

Lobreaux, S., Massenet, O., and Briat, J.F. (1992). Iron induces ferritin synthesis in maize plantlets. Plant Mol. Biol. **19,** 563–575.

Long, J.A., and Barton, M.K. (1998). The development of apical embryonic pattern in Arabidopsis. Development **125,** 3027–3035.

Long, J.A., Moan, E.I., Medford, J.I., and Barton, M.K. (1996). A member of the KNOTTED class of homeodomain proteins encoded by the STM gene of Arabidopsis. Nature **379,** 66–69.

MacDiarmid, C.W., and Eide, D.J. (2001). Metals and Cells, abstract C1.52. (Canterbury, UK: Society of Experimental Biology). Available at www.ncl.ac.uk/sbg/robinson/abstracts.html.

Marschner, H., and Röhmeld, V. (1994). Strategies of plants for acquisition of iron. Plant Soil **165,** 375–388.

Murashige, T., and Skoog, F. (1962). A revised medium for rapid growth and bioassays with tobacco tissue cultures. Physiol. Plant. **15,** 473–497.

Nakai, K., and Kanehisa, M. (1992). A knowledge base for predicting protein localization sites in eukaryotic cells. Genomics **14,** 897–911.

Pich, A., Manteuffel, R., Hillmer, S., Scholz, G., and Schmidt, W. (2001). Fe homeostasis in plant cells: Does nicotianamine play multiple roles in the regulation of cytoplasmic Fe concentration? Planta **213,** 967–976.

Robinson, N.J., Procter, C.M., Connolly, E.L., and Guerinot, M.L. (1999). A ferric-chelate reductase for iron uptake from soils. Nature **397,** 694–697.

Robinson, N.J., Sadjuga, and Groom, Q.J. (1997). The froh gene family from *Arabidopsis thaliana*: Putative iron-chelate reductases. Plant Soil **196,** 245–248.

Rogers, E.E., Eide, D.J., and Guerinot, M.L. (2000). Altered selectivity in an Arabidopsis metal transporter. Proc. Natl. Acad. Sci. USA **97,** 12356–12360.

Sambrook, J., Fritsch, E., and Maniatis, T. (1989). Molecular Cloning: A Laboratory Manual. (Cold Spring Harbor, NY: Cold Spring Harbor Laboratory Press).

Schirawski, J., Planchais, S., and Haenni, A.L. (2000). An improved protocol for the preparation of protoplasts from an established *Arabidopsis thaliana* cell suspension culture and infection with RNA of turnip yellow mosaic tymovirus: A simple and reliable method. J. Virol. Methods **86,** 85–94.

Stephan, U.W., and Scholz, G. (1993). Nicotianamine: Mediator of transport of iron and heavy metals in the phloem. Physiol. Plant. **88,** 522–529.

Takagi, S.I., Nomoto, K., and Takemoto, T. (1984). Physiological aspect of mugineic acid, a possible phytosiderophore of graminaceous plants. J. Plant Nutr. **7,** 1–5.

Taketani, S., and Tokunaga, R. (1982). Purification and substrate specificity of bovine liver-ferrochelatase. Eur. J. Biochem. **127,** 443–447.

Thomine, S., Wang, R., Ward, J.M., Crawford, N.M., and Schroeder, J.I. (2000). Cadmium and iron transport by members of a plant metal transporter family in Arabidopsis with homology to Nramp genes. Proc. Natl. Acad. Sci. USA **97,** 4991–4996.

Touraine, B., and Glass, A.D. (1997). NO_3^- and ClO_3^- fluxes in the chl1-5 mutant of *Arabidopsis thaliana*: Does the CHL1-5 gene encode a low-affinity NO_3^- transporter? Plant Physiol. **114,** 137–144.

Vert, G., Briat, J.F., and Curie, C. (2001). Arabidopsis IRT2 gene encodes a root-periphery iron transporter. Plant J. **26,** 181–189.

Welch, R.M., Norvell, W.A., Schaefer, S.C., Shaff, J.E., and Kochian, L.V. (1993). Induction of iron (III) and copper (II) reduction in pea (*Pisum sativum* L.) roots by Fe and Cu status: Does the root-cell plasmalemma Fe(III)-chelate reductase perform a general role in regulating cation uptake? Planta **190,** 555–561.